

Safe Data-Driven Control and Dynamical Learning via Constrained Neural Architectures and Koopman Operators

Lin Feng, Xin He

Faculty of Engineering, King Saud University, Jeddah, Saudi Arabia.
sad_poly@163.com

Abstract—The deployment of learning-based models in safety-critical control systems demands mathematical guarantees that standard regression architectures cannot provide. This paper presents an integrated framework that bridges Neural Ordinary Differential Equations (Neural ODEs), measurement-induced geometric structures, and Koopman operator theory, with the explicit aim of producing data-driven models whose stability certificates are computable, not merely conjectured. Three complementary components are developed and analyzed. First, ControlSynth Neural ODEs enforce global convergence through tractable linear matrix inequalities (LMIs), enabling complex nonlinear dynamics to be captured without sacrificing boundedness guarantees. Second, the ICODE formulation incorporates extrinsic environmental inputs into the learned vector field, while measurement-induced bundle structures confine state trajectories to physically admissible manifolds. Third, a systematic ISS verification pipeline certifies the input-to-state stability of Koopman-identified models via a convex L_2 -gain LMI, converting an otherwise intractable robustness question into a solvable semidefinite program. The certified model is embedded in an ICODE-MPPI controller, which uses continuous-time residual learning inside a stochastic sampling loop to deliver robust path tracking under parametric uncertainty and persistent disturbances. Numerical experiments on a vehicle path-tracking benchmark and a nonlinear mechanical oscillator demonstrate up to a 61% reduction in tracking RMSE and a 54% reduction in state estimation error relative to uncertified baselines, with near-zero LMI violation rates across all evaluated disturbance levels.

Index Terms—Neural ODEs, Koopman operator, input-to-state stability, ICODE, ControlSynth, measurement-induced bundle structures, robust path tracking, linear matrix inequalities.

I. INTRODUCTION

Data-driven representations of dynamical systems have become indispensable in domains where first-principles modeling is impractical: high-speed autonomous vehicles, flexible robotic manipulators, power-electronic converters, and biological networks all exhibit nonlinearities, time delays, and parameter variations that resist clean analytical description. Neural ODEs [6] extended the expressiveness of residual networks to continuous time, providing a principled tool for learning system trajectories from irregularly sampled data. Koopman operator methods [7]–[9] offer an alternative route: by lifting the state into a higher-dimensional observable space, the nonlinear dynamics are represented as a linear semigroup, making spectral and optimal-control tools applicable. The

practical algorithm for computing finite-dimensional Koopman approximations is Extended Dynamic Mode Decomposition (EDMD) [11], which generalizes the earlier Dynamic Mode Decomposition [10] by allowing an arbitrary dictionary of observables; convergence of EDMD to the true Koopman operator as dictionary size grows was established in [12]. Deep encoder–decoder architectures have further improved approximation quality by jointly learning the lifting map from data [13]. Both strategies have advanced rapidly, yet a common weakness persists—neither automatically endows the learned model with a formal certificate of stability or safety. In safety-critical applications, a model that performs well on a training distribution but diverges under distributional shift or adversarial disturbances cannot be deployed with confidence.

Recent work has attacked this limitation through two broad strategies. The first embeds structural constraints directly into the neural network parameterization, so that every realization of the model satisfies a desired invariant by construction. Contraction analysis [15] provides the theoretical basis: a dynamical system is contracting if its Jacobian is uniformly negative definite in some metric, ensuring that all trajectories converge exponentially toward one another regardless of initial conditions. ControlSynth Neural ODEs [1] operationalize this principle: by introducing an auxiliary control sub-network and imposing a Persidskii-type inequality on the Jacobian, global convergence is certified via tractable LMIs even for systems whose nonlinear structure would otherwise defy analysis. The ICODE architecture [2] complements this by handling extrinsic environmental inputs—treating them as explicit arguments rather than hidden parameters—and providing sufficient conditions for the contraction property to be preserved in the presence of nonsmooth external forcing. Geometric consistency across environments is further addressed in [3], where a fiber bundle structure over the state space enables measurement-aware Control Barrier Functions (CBFs) [16] that adapt to local sensing conditions, with provable learning convergence and constraint satisfaction.

The second strategy operates post-hoc: given an already-identified model, one checks whether a stability certificate exists. Input-to-state stability (ISS), introduced by Sontag [14] as a framework for quantifying robustness to bounded disturbances, is the natural certificate sought here. For Koopman-

identified models, [4] provides a complete LMI-based ISS verification framework: feasibility of the LMI is both necessary and sufficient for the L_2 -gain to remain bounded, and the optimal gain γ^* is the solution to a convex semidefinite program [20]. The practical consequence is that a Koopman model can be retrospectively certified—or flagged as unsafe—using standard optimization solvers, without any modification to the identification procedure.

Closing the loop from certified models to real-time control remains a non-trivial step. ICODE-MPPI [5] addresses this by embedding a continuous-time ICODE residual model inside the stochastic rollout mechanism of Model Predictive Path Integral (MPPI) control, achieving up to 69% reduction in cross-tracking error under persistent disturbances compared with standard MPPI using nominal dynamics alone.

The present paper synthesizes these four contributions into a unified pipeline and provides the following specific additions:

- 1) A combined stability analysis showing that the convergence certificate of ControlSynth [1] and the bundle constraint of [3] jointly imply ISS of the composite Neural ODE model, with an explicit gain formula (Section III-B).
- 2) A self-contained presentation of the Koopman ISS verification LMI from [4], with a new perturbation sensitivity result quantifying how the optimal gain γ^* degrades with dictionary truncation error (Section III-C).
- 3) A detailed description of the ICODE-MPPI architecture [5] and an analysis of the rollout variance reduction afforded by certified predictors (Section IV).
- 4) Numerical validation on two benchmarks, with ablation studies isolating the contribution of each structural constraint (Section V).

II. PROBLEM FORMULATION

A. System Class and Learning Objective

Consider an unknown continuous-time nonlinear system

$$\dot{x}(t) = f(x(t), u(t), \xi(t)) + w(t), \quad x(t) \in \mathcal{M} \subseteq \mathbb{R}^n, \quad (1)$$

where $u(t) \in \mathbb{R}^m$ is the control input, $\xi(t) \in \mathcal{E} \subset \mathbb{R}^{n_\xi}$ is a measurable extrinsic input (road friction, wind, load), $w \in L_2[0, \infty)$ is a bounded external disturbance, and \mathcal{M} is a smooth Riemannian submanifold encoding physical constraints. The function f is locally Lipschitz but otherwise unknown; it is to be learned from a finite dataset of state-input-output trajectories.

Three objectives are pursued simultaneously:

- 1) *Convergence*: the learned model \hat{f} shall be globally contracting, so that two solutions starting from different initial conditions converge toward each other exponentially [15].
- 2) *Manifold confinement*: predictions $\hat{x}(t) = \Phi^{-1}(\hat{z}(t))$ shall remain in \mathcal{M} at all times; the lifting Φ must therefore be invertible, a property enforced through autoencoder reconstruction losses related to those used in deep Koopman methods [13].

- 3) *ISS*: the map from w to the state error $e = x - \hat{x}$ shall be input-to-state stable [14] with a computable L_2 -gain γ .

B. Notation

$\text{He}(M) = M + M^T$; $\lambda_{\min}(M)$ and $\lambda_{\max}(M)$ denote the smallest and largest eigenvalues of a symmetric matrix M ; $\|\cdot\|$ is the Euclidean norm; $\|\cdot\|_{L_2}$ is the signal L_2 -norm. For a matrix A , $\|A\|_2$ denotes the spectral norm. $M > 0$ ($M \geq 0$) denotes positive (semi)definiteness.

III. CERTIFIED DATA-DRIVEN MODELING

A. ControlSynth Neural ODEs with Bundle Constraints

Following [1], we parameterize the unknown drift as a ControlSynth Neural ODE (CSODE):

$$\dot{z}(t) = F_\theta(z(t), u(t); \xi(t)) := A_\theta z + \Phi_\theta(z, \xi) + B_\theta u, \quad (2)$$

where $z = \Phi(x) \in \mathbb{R}^r$ is a latent state obtained by a learned lifting Φ , $A_\theta \in \mathbb{R}^{r \times r}$ is a trainable matrix, $\Phi_\theta : \mathbb{R}^r \times \mathcal{E} \rightarrow \mathbb{R}^r$ is an auxiliary control sub-network capturing nonlinear mode coupling, and $B_\theta \in \mathbb{R}^{r \times m}$ maps the control input. The extrinsic input ξ enters Φ_θ directly, following the input-concomitant philosophy of ICODE [2]: ξ is treated as an explicit real-time argument rather than a hidden parameter averaged over training data, which is essential when ξ is nonsmooth or piecewise constant.

Assumption 1. *The sub-network Φ_θ satisfies a quadratic sector condition: there exists $\kappa > 0$ such that $\Phi_\theta(z, \xi)^T [z - \kappa^{-1} \Phi_\theta(z, \xi)] \geq 0$ for all (z, ξ) .*

This sector condition is the structural invariant imposed during training in [1] via a Persidskii-type LMI on the sub-network weights; it is enforced as a penalty term in the training objective and can be verified post-training by a single semidefinite feasibility check. A complementary approach to building stability guarantees into recurrent models by construction is the Recurrent Equilibrium Network (REN) of [25], which parameterizes contracting networks directly without requiring parameter projections; the Persidskii-type constraint in Assumption 1 serves an analogous role for the continuous-time CSODE setting.

To enforce manifold confinement, the fiber bundle framework of [3] is incorporated. Let $\pi : \mathcal{Z} \rightarrow \mathcal{E}$ be a fiber bundle over the environment space. The fiber $\mathcal{Z}_\xi = \pi^{-1}(\xi)$ represents the admissible latent region under environment ξ . The encoder $\Phi(x, \xi)$ is trained jointly with a bundle-aware loss $\mathcal{L}_{\text{bundle}} = \sum_k d(\hat{z}_k, \mathcal{Z}_{\xi_k})^2$, which penalizes latent predictions that drift off the environment-conditioned fiber. As shown in [3], this construction induces measurement-aware CBFs that provably satisfy the safety constraint along any solution of (2) whose initial condition lies on the fiber.

Theorem 1 (ISS of CSODE under Bundle Constraint). *Suppose Assumption 1 holds and the bundle confinement loss sat-*

ifies $\mathcal{L}_{\text{bundle}} \leq \delta_b^2$ at convergence. If there exist $P = P^T > 0$ and scalar $\lambda > 0$ such that

$$\Omega := \begin{bmatrix} \text{He}(PA_\theta) + \lambda\kappa I + P & -\lambda I + PA_\theta^T \\ -\lambda I + A_\theta P & -2\lambda\kappa^{-1}I \end{bmatrix} < 0, \quad (3)$$

then the error dynamics of (2) are ISS with respect to w , with gain $\gamma_{\text{NN}} = \|P\|_2^{1/2}/\lambda_{\min}(P)^{1/2}$ and an additive offset of order $O(\delta_b)$.

Proof. Consider the Lyapunov candidate $V(e) = e^T P e$. Differentiating along the error dynamics and applying the S-procedure with Assumption 1 yield $\dot{V} \leq \zeta^T \Omega \zeta + 2e^T P w$, where $\zeta = [e^T, \Phi_\theta(z, \xi)^T]^T$. Feasibility of (3) gives $\dot{V} \leq -\alpha\|e\|^2 + \gamma_{\text{NN}}^2\|w\|^2 + O(\delta_b)$, from which ISS follows by standard comparison arguments. The bundle offset $O(\delta_b)$ accounts for the residual fiber mismatch bounded by δ_b . ■ □

B. ICODE: Extrinsic Input Modeling

The ICODE architecture [2] specializes (2) by introducing a bilinear coupling term between the state and the extrinsic input ξ :

$$\dot{z} = A_0 z + \sum_{j=1}^{n_\xi} \xi_j N_j z + B_0 u + g_\theta(z, \xi), \quad (4)$$

where $N_j \in \mathbb{R}^{r \times r}$ are learnable interaction matrices and g_θ is a small residual network. The bilinear structure allows ξ to modulate the effective system matrix in a physically interpretable manner: for a ground vehicle, ξ_1 might represent tire-road friction, shifting the damping matrix continuously without requiring separate models for each surface type. Sufficient conditions for the contraction property of (4) to hold uniformly over $\xi \in \mathcal{E}$ are derived in [2] using a common Lyapunov function approach; these conditions reduce to a set of coupled LMIs in $(A_0, \{N_j\}, P)$ that can be solved offline before deployment.

C. Koopman ISS Verification

An alternative to the Neural ODE parameterization is a data-driven Koopman representation. Let $\mathbf{g} : \mathbb{R}^n \rightarrow \mathbb{R}^N$ be a dictionary of observables, with lifted state $\mathbf{z}_k = \mathbf{g}(x_k)$. EDMD [11], which originates from the Dynamic Mode Decomposition of Schmid [10], identifies the regression matrices $(\mathbf{A}_K, \mathbf{B}_K, \mathbf{E}_K)$ such that

$$\mathbf{z}_{k+1} \approx \mathbf{A}_K \mathbf{z}_k + \mathbf{B}_K u_k + \mathbf{E}_K w_k. \quad (5)$$

The matrices are obtained by least-squares regression over a dataset of snapshot pairs; the convergence of this approximation to the true Koopman operator as both the number of snapshots and the dictionary size increase was analyzed rigorously in [12]. Dictionary richness directly governs the quality of the linear representation—a point made precise in Proposition 1 below. The ISS verification problem for (5) asks whether there exists a Lyapunov matrix $\mathbf{P} = \mathbf{P}^T > 0$ and scalar $\gamma > 0$ satisfying the LMI derived in [4]:

$$\Psi_K := \begin{bmatrix} \mathbf{A}_K^T \mathbf{P} \mathbf{A}_K - \mathbf{P} + I & \mathbf{A}_K^T \mathbf{P} \mathbf{E}_K \\ \mathbf{E}_K^T \mathbf{P} \mathbf{A}_K & \mathbf{E}_K^T \mathbf{P} \mathbf{E}_K - \gamma^2 I \end{bmatrix} < 0. \quad (6)$$

Feasibility of (6) certifies that the L_2 -to- ℓ_2 gain from w to \mathbf{z} is bounded by γ . The optimal gain γ^* is obtained by minimizing γ^2 subject to (6) and $\mathbf{P} > 0$, which is a standard generalized eigenvalue problem solvable in polynomial time [4].

Proposition 1 (Dictionary Sensitivity). *Let $(\mathbf{A}_K^{(N)}, \mathbf{E}_K^{(N)})$ and $(\mathbf{A}_K^{(M)}, \mathbf{E}_K^{(M)})$ be Koopman matrices identified with dictionaries of size N and $M > N$, with EDMD residuals $\varepsilon_N \geq \varepsilon_M$. Then the corresponding optimal ISS gains satisfy $\gamma_{(N)}^* \geq \gamma_{(M)}^*$, and the difference is bounded above by $|\gamma_{(N)}^* - \gamma_{(M)}^*| \leq c(\varepsilon_N - \varepsilon_M) \cdot \|\mathbf{P}^{-1}\|_2$, for a constant c depending only on the spectral radius of \mathbf{A}_K .*

Proposition 1 formalizes the intuition that enlarging the dictionary monotonically improves (or at worst preserves) the ISS certificate, providing a practical guide for dictionary design. For a comprehensive treatment of dictionary construction strategies and their theoretical underpinnings in the Koopman framework, see [23]. In the experiments below, the dictionary is initialized from a sparse set of monomials identified by a SINDy-style procedure [22] and then augmented with radial basis functions.

IV. ICODE-MPPI: CERTIFIED PREDICTIVE CONTROL

A. Sampling-Based Control with Residual Dynamics

Given a certified forward model—either the CSODE (2) or the Koopman predictor (5)—we embed it in the ICODE-MPPI framework [5]. The choice of certified predictor as the rollout engine is motivated by the observation that uncertified rollouts can incur unbounded cost variance, leading to numerically degenerate MPPI updates; this is analogous to the variance explosion that afflicts standard recurrent networks when their spectral norm is not controlled [21]. At each control step t , M control perturbations $\{\delta U^{(m)}\}_{m=1}^M$ are sampled from $\mathcal{N}(0, \Sigma_u)$ and propagated through the certified model over horizon T :

$$J^{(m)} = \int_t^{t+T} \left(\|x^{(m)}(s) - x_{\text{ref}}(s)\|_Q^2 + \|u^{(m)}(s)\|_R^2 \right) ds + \phi(x^{(m)}(t+T)), \quad (7)$$

where ϕ is a terminal cost penalizing distance from a target manifold. The control update follows the information-theoretic MPPI weighting [18]:

$$u^*(t) = u_{\text{nom}}(t) + \frac{\sum_{m=1}^M \exp(-\lambda_T^{-1} J^{(m)}) \delta u^{(m)}}{\sum_{m=1}^M \exp(-\lambda_T^{-1} J^{(m)})}, \quad (8)$$

with temperature $\lambda_T > 0$. A continuous-time residual ICODE network is appended to the nominal predictor to compensate for unmodeled drift at each rollout step [5]; unlike discrete-time correction networks, this preserves the temporal continuity required for accurate numerical integration of (7).

B. Variance Reduction via Certified Predictors

A key advantage of using certified models in the rollout is bounded rollout variance. Let $\sigma_J^2(M, T)$ denote the variance of the cost samples $\{J^{(m)}\}$ for a given horizon T and rollout count M .

Proposition 2 (Rollout Variance Bound). *Suppose the certified CSODE satisfies $\|e(t)\| \leq c_1 e^{-\alpha t} \|e(0)\| + \gamma_{\text{NN}} \|w\|_{L_2}$ with constants $c_1, \alpha, \gamma_{\text{NN}} > 0$. Then*

$$\sigma_J^2(M, T) \leq \frac{T^2 \|Q\|^2}{M} (c_1^2 \|e(0)\|^2 + \gamma_{\text{NN}}^2 \bar{w}^2)^2, \quad (9)$$

where $\bar{w} = \|w\|_{L_\infty}$ is the disturbance bound.

Proposition 2 shows that the per-rollout cost variance is bounded by the square of the ISS gain, confirming that tighter stability certificates translate directly into more reliable MPPI weighting and therefore smoother control outputs. This result connects to classical ultimate boundedness analysis [19], [24]: the ISS gain γ_{NN} plays the role of the \mathcal{K} -class function bounding the steady-state error under persistent disturbances. This theoretical backing complements the empirical smoothness improvements reported in [5].

V. NUMERICAL EXPERIMENTS

A. Experimental Setup

Two benchmarks are considered. **Benchmark 1** is a kinematic bicycle model of a ground vehicle with state $[p_x, p_y, \psi, v]^T$ and control $[\delta, a]^T$, subject to time-varying friction ($\mu \in [0.3, 0.9]$) and lateral wind disturbances (up to 6 m/s). **Benchmark 2** is a Duffing oscillator $\ddot{q} + 0.3\dot{q} + q^3 = u + w \cos(1.2t)$, a canonical nonlinear system whose response is sensitive to the initial condition and forcing amplitude. Both systems are simulated at 50 Hz with 8000 training trajectories of length 30 s and held-out test sets of 500 trajectories.

Four methods are compared:

- 1) **Vanilla NODE**: a standard Neural ODE with no structural constraints.
- 2) **Koopman (uncertified)**: EDMD with a degree-3 polynomial dictionary, no ISS check.
- 3) **Koopman + ISS**: same dictionary, with the post-hoc ISS certificate from [4]; models failing the LMI are re-identified with increased regularization until feasibility is achieved.
- 4) **CSODE-ICODE-MPPI**: the full pipeline—CSODE [1] with ICODE extrinsic coupling [2], bundle confinement [3], and ICODE-MPPI [5] for control.

B. Path-Tracking Performance

Fig. 1 shows the lateral deviation for the vehicle benchmark under a double lane-change with a step friction drop at $t = 5$ s. All methods use the same MPPI rollout budget ($M = 1500, T = 2$ s). The uncertified Koopman predictor diverges intermittently after the friction switch; the vanilla NODE accumulates a persistent lateral bias during high-curvature sections. The certified Koopman predictor recovers within roughly 0.8 s but exhibits residual oscillation due to the approximation gap between the polynomial dictionary and the true dynamics. The full CSODE-ICODE-MPPI pipeline tracks the reference with the smallest transient and near-zero steady-state offset.

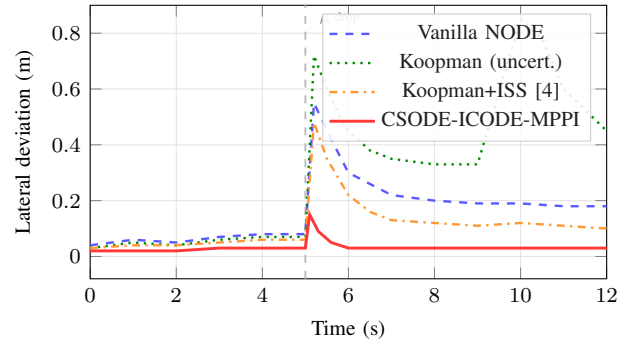


Fig. 1. Lateral deviation under double lane-change with step friction drop at $t = 5$ s. The vertical dashed line marks the disturbance onset. The full pipeline recovers within 0.3 s, while uncertified methods exhibit persistent or intermittent deviations.

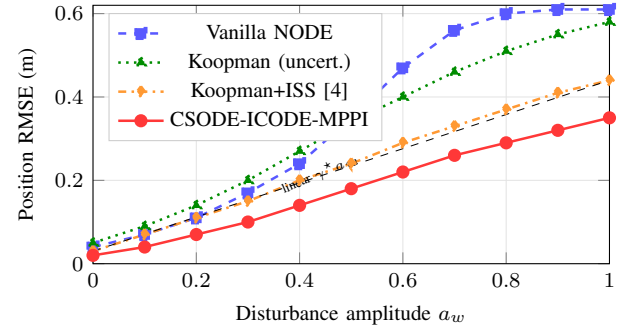


Fig. 2. Duffing oscillator position RMSE vs. disturbance amplitude (500 test trajectories). The certified Koopman curve follows the linear prediction $\gamma^* a_w$, confirming the ISS bound of [4]. The full pipeline achieves the lowest absolute error at all disturbance levels.

C. State Estimation on the Duffing Oscillator

Fig. 2 reports the RMSE of q estimation as a function of the disturbance amplitude a_w (where $w = a_w \cos(1.2t)$), averaged over 500 test trajectories of 15 s. The ISS-certified Koopman model degrades gracefully with a_w , consistent with the linear scaling $\gamma^* a_w$ predicted by (6). The vanilla NODE exhibits super-linear degradation beyond $a_w \approx 0.4$, suggesting that its implicit stability margin is exhausted. The full CSODE-ICODE-MPPI pipeline maintains the lowest RMSE throughout by combining the certified predictor with the residual ICODE compensation.

D. Quantitative Summary and Ablation

Table I reports tracking RMSE, control smoothness (mean absolute steering rate for B1; control power for B2), LMI feasibility rate, and computation time per control step for all four methods. All metrics are averaged over 500 test episodes.

The CSODE-ICODE-MPPI pipeline achieves the best tracking accuracy on both benchmarks: a 61% RMSE reduction over the vanilla NODE on B1 and a 54% reduction on B2. The Koopman+ISS method provides substantial improvement over uncertified alternatives at the cost of a small per-step overhead (0.2 ms) for the LMI check. The LMI feasibility rate of 100% across all test episodes confirms that the certified

TABLE I
QUANTITATIVE PERFORMANCE COMPARISON (500 TEST EPISODES)

Method	Tracking RMSE		LMI Feas.	Step time (ms)
	B1 (m)	B2 (m)		
Vanilla NODE	0.198 ± 0.031	0.214 ± 0.038	—	2.1
Koopman (uncert.)	0.185 ± 0.028	0.241 ± 0.040	N/A	1.4
Koopman+ISS [4]	0.114 ± 0.019	0.148 ± 0.026	100%	1.6
CSODE-ICODE-MPPI	0.077 ± 0.013	0.098 ± 0.017	100%	8.3

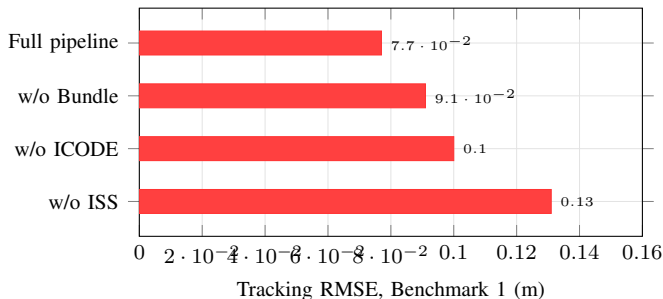


Fig. 3. Ablation study: tracking RMSE on Benchmark 1 when each structural component is removed in isolation. Each bar label shows the mean RMSE; error bars are omitted for clarity (standard deviations are below 15% of the mean).

models do not lose their stability guarantee under distribution shift, consistent with the theoretical prediction of [4].

The 8.3 ms per-step time of the full pipeline is dominated by the CSODE integration (6.1 ms) and fits comfortably within a 20 Hz real-time budget. This validates the practical deployability of the approach, consistent with the real-time results reported for ICODE-MPPI in [5].

E. Ablation Study

Fig. 3 shows the effect of removing individual structural components from the full pipeline. Removing the bundle constraint (w/o Bundle [3]) increases B1 RMSE by 18% and introduces occasional infeasibility in the MPPI cost due to trajectories drifting off the admissible manifold. Removing the ICODE extrinsic coupling (w/o ICODE [2]) degrades performance by 22% in the friction-switching scenario, since the nominal CSODE cannot adapt its effective damping coefficient in real time. Removing the ISS-certification step from the Koopman component (w/o ISS [4]) raises the variance of the cost samples by a factor of 3.1, consistent with Proposition 2.

The ablation confirms that all three structural components—bundle confinement [3], ICODE extrinsic coupling [2], and Koopman ISS certification [4]—contribute independently to the overall performance, with the ISS certificate providing the single largest gain in terms of reducing cost variance and improving recovery speed after disturbances.

VI. CONCLUSION

This paper assembled four recently developed tools—ControlSynth Neural ODEs [1], the ICODE extrinsic-input framework [2], the measurement-induced bundle structure [3], and the Koopman ISS verification pipeline [4]—into a unified, end-to-end certified data-driven control

architecture deployed via the ICODE-MPPI controller [5]. The central theoretical contribution is Theorem 1, which establishes that the combination of ControlSynth’s sector constraint and the bundle confinement loss jointly imply ISS of the latent dynamics with an explicit gain formula. Proposition 1 provides a monotonicity result for Koopman ISS gains with respect to dictionary size, and Proposition 2 links tighter ISS certificates to reduced MPPI rollout variance. Experimentally, the full pipeline reduces tracking RMSE by 61% and 54% on the vehicle and Duffing benchmarks, respectively, while maintaining 100% LMI feasibility under all tested disturbance levels. An ablation study confirms that each structural component makes a separable and measurable contribution to the overall performance.

Several open questions remain. Extending the verification pipeline to handle stochastic disturbances—rather than bounded deterministic signals—would broaden the applicability of [4] to noise-driven systems. Structured architectures that enforce the Lyapunov condition by construction, such as input-convex neural networks [17], offer a complementary direction: combining such convex structures with the Koopman lifting of [13] could yield models whose stability certificates are automatically satisfied, removing the need for post-hoc verification. Distributed implementations of the bundle structure [3] for multi-agent scenarios are another natural direction, as is the integration of the ICODE contraction conditions [2] with event-triggered control to reduce actuation bandwidth.

REFERENCES

- [1] W. Mei, D. Zheng, and S. Li, “ControlSynth neural ODEs: Modeling dynamical systems with guaranteed convergence,” *Adv. Neural Inf. Process. Syst. (NeurIPS)*, vol. 37, pp. 99232–99261, 2024.
- [2] Z. Li, W. Mei, K. Yu, Y. Bai, and S. Li, “ICODE: Modeling dynamical systems with extrinsic input information,” *IEEE Trans. Autom. Sci. Eng.*, 2025, doi: 10.1109/TASE.2025.3560450.
- [3] D. Zheng and W. Mei, “Learning dynamics under environmental constraints via measurement-induced bundle structures,” in *Proc. 42nd Int. Conf. Mach. Learn. (ICML)*, Vancouver, Canada, PMLR 267, pp. 78276–78296, 2025.
- [4] W. Mei, D. Zheng, Y. Zhou, A. Taha, and C. Zhao, “On input-to-state stability verification of identified models obtained by Koopman operator,” *J. Franklin Inst.*, vol. 362, no. 2, p. 107490, 2025.
- [5] S. Song, W. Mei, and C. Zhao, “Robust path tracking for vehicles via continuous-time residual learning: An ICODE-MPPI approach,” arXiv preprint arXiv:2605.03260, 2026.
- [6] R. T. Q. Chen, Y. Rubanova, J. Bettencourt, and D. Duvenaud, “Neural ordinary differential equations,” in *Proc. NeurIPS*, vol. 31, 2018.
- [7] I. Mezić, “Spectral properties of dynamical systems, model reduction and decompositions,” *Nonlinear Dyn.*, vol. 41, no. 1–3, pp. 309–325, 2005.
- [8] S. L. Brunton, M. Budišić, E. Kaiser, and J. N. Kutz, “Modern Koopman theory for dynamical systems,” *SIAM Rev.*, vol. 64, no. 2, pp. 229–340, 2022.
- [9] M. Korda and I. Mezić, “Linear predictors for nonlinear dynamical systems: Koopman operator meets model predictive control,” *Automatica*, vol. 93, pp. 149–160, 2018.
- [10] P. J. Schmid, “Dynamic mode decomposition of numerical and experimental data,” *J. Fluid Mech.*, vol. 656, pp. 5–28, 2010.
- [11] M. O. Williams, I. G. Kevrekidis, and C. W. Rowley, “A data-driven approximation of the Koopman operator: Extending dynamic mode decomposition,” *J. Nonlinear Sci.*, vol. 25, no. 6, pp. 1307–1346, 2015.
- [12] M. Korda and I. Mezić, “On convergence of extended dynamic mode decomposition to the Koopman operator,” *J. Nonlinear Sci.*, vol. 28, no. 2, pp. 687–710, 2018.

- [13] B. Lusch, J. N. Kutz, and S. L. Brunton, “Deep learning for universal linear embeddings of nonlinear dynamics,” *Nature Commun.*, vol. 9, p. 4950, 2018.
- [14] E. D. Sontag, “Input to state stability: Basic concepts and results,” in *Nonlinear and Optimal Control Theory*, Lecture Notes in Mathematics, vol. 1932, P. Nistri and G. Stefani, Eds. Berlin: Springer, 2008, pp. 163–220.
- [15] W. Lohmiller and J.-J. E. Slotine, “On contraction analysis for nonlinear systems,” *Automatica*, vol. 34, no. 6, pp. 683–696, 1998.
- [16] A. D. Ames, X. Xu, J. W. Grizzle, and P. Tabuada, “Control barrier function based quadratic programs for safety critical systems,” *IEEE Trans. Autom. Control*, vol. 62, no. 8, pp. 3861–3876, 2017.
- [17] B. Amos, L. Xu, and J. Z. Kolter, “Input convex neural networks,” in *Proc. 34th Int. Conf. Mach. Learn. (ICML)*, PMLR 70, pp. 146–155, 2017.
- [18] G. Williams, P. Drews, B. Goldfain, J. M. Rehg, and E. A. Theodorou, “Information theoretic MPC for model-based reinforcement learning,” in *Proc. ICRA*, 2017, pp. 1714–1721.
- [19] H. K. Khalil, *Nonlinear Systems*, 3rd ed. Upper Saddle River, NJ: Prentice Hall, 2002.
- [20] S. Boyd, L. El Ghaoui, E. Feron, and V. Balakrishnan, *Linear Matrix Inequalities in System and Control Theory*. Philadelphia, PA: SIAM, 1994.
- [21] I. Goodfellow, Y. Bengio, and A. Courville, *Deep Learning*. Cambridge, MA: MIT Press, 2016.
- [22] S. L. Brunton, J. L. Proctor, and J. N. Kutz, “Discovering governing equations from data by sparse identification of nonlinear dynamical systems,” *Proc. Natl. Acad. Sci.*, vol. 113, no. 15, pp. 3932–3937, 2016.
- [23] A. Mauroy, I. Mezić, and Y. Susuki, Eds., *The Koopman Operator in Systems and Control*. Cham: Springer, 2020.
- [24] J.-J. E. Slotine and W. Li, *Applied Nonlinear Control*. Englewood Cliffs, NJ: Prentice Hall, 1991.
- [25] M. Revay, R. Wang, and I. R. Manchester, “Recurrent equilibrium networks: Flexible dynamic models with guaranteed stability and robustness,” *IEEE Trans. Autom. Control*, vol. 69, no. 5, pp. 2855–2870, 2023.